Modified solution-processible fabrication of metallic photonic crystals with template removal

Hongmei Liu (刘红梅), Xinping Zhang (张新平)*, Jingjuan Li (李景娟), and Jiaoyang Song (宋骄阳)

College of Applied Sciences, Beijing University of Technology, Beijing 100124, China

**E-mail: zhangxinping@bjut.edu.cn*

Received July 14, 2009

High-temperature annealing and pre-annealing lift-off procedures are employed to improve the solution-processible technique for the fabrication of one- (1D) and two-dimensional (2D) metallic photonic crystals (MPCs) based on colloidal gold nanoparticles. This enables the successful fabrication of gold nanowires or nanocylinder array structures with the photoresist template removed completely, which is crucial for the application of MPCs in biosensors and optoelectronic devices. Microscopic measurements show homogeneous 1D and 2D photonic structures with an area as large as 100 mm^2. Plasmonic resonance of the gold nanostructures and its coupling with the resonance mode of the planar waveguide underneath the photonic structures are observed, implying the excellent optical properties of this kind of MPCs based on the improved fabrication technique.

OCIS codes: 050.6624, 160.4236, 160.5298, 240.6680.

doi: 10.3788/COL20090710.0912.

Metallic photonic crystals (MPCs) are attractive for their special photoelectronic properties and potential applications in optical polarizers[1], optical filters[2], all-optical switches[3], distributed feed-back lasers, and sensors[4]. A number of techniques are available for the fabrication of MPCs, including those based on electron beam lithography (EBL)[5,6], nano-imprinting lithography (NIL)[7−9], focused ion beam (FIB) lithography[10−13], etc. Solution-processible method enables simple, low-cost, and mass fabrication of MPCs[14−16], where the photoresist grating template does not need to be removed, which improves the stability and reproducibility of the fabrication significantly and is considered as a big advantage of this technique. However, the photoresist may sometimes introduce disturbance in the application of MPCs in biosensors and some optoelectronic devices. Thus, removal of the photoresist template becomes crucial in some cases. In this letter, we report two kinds of methods to produce the one- (1D) and two-dimensional (2D) MPCs using gold nanoparticles in colloidal solution with the photoresist successfully removed, where we employ "high-temperature annealing" and "pre-annealing lift-off processes", respectively.

In the first step of fabrication, a photoresist nanograting is fabricated on the top of an indium tin oxide (ITO) layer deposited on a glass substrate with an area as large as 100 mm^2 using interference lithography. The colloidal suspension of gold nanoparticles is then spin-coated onto the photoresist grating template, so that the gold nanoparticles are mainly confined into the grating grooves due to the surface energy difference between the photoresist and the ITO[15]. The synthesis of the gold nanoparticles is detailed in Ref. [17], and the size of the nanoparticles is in the range of 2–8 nm in diameter. The ITO waveguide is 200 nm in thickness, deposited on a 1-mm-thick glass substrate. Both the positive photoresist S1805 and the negative photoresist SU8 have been used to fabricate different gold structures, as will be indicated separately later.

In the "high-temperature annealing" process, the sample is processed as follows. The sample prepared in the first step is put into a muffle furnace that is set at 300 °C and annealed for 1 min; the temperature of the furnace is then increased to 450 °C, which is kept constant for 15–20 min. During the annealing process, both the photoresist and the organic ligands on the gold nanoparticles are burnt off while the gold nanopartilces become melted and form excellent nanostructures. The high surface energy of the molten gold has played an important role in the self-assembly of the gold into the patterned structures.

Figures 1(a) and (b) show the atomic force microscopic (AFM) images of the 1D and 2D MPCs fabricated using the high-temperature annealing method, where the negative photoresist SU8 is used to fabricate the template grating structures. It can be seen clearly in Fig. 1(a) that the 1D MPC becomes broken, forming randomly distributed gold nano-islands. Whereas in the 1D structures, the photoresist template grating controls the periodic arrangement of the gold nano-islands, forming gold nanograting structures in the direction perpendicular to the template grating grooves. The 1D nano-island arrays have the same period of about 330 nm as the

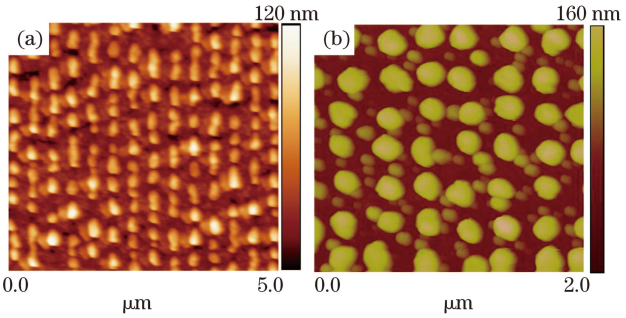

Fig. 1. AFM images of (a) 1D and (b) 2D gold photonic crystals with the photoresist mask grating removed through "high-temperature annealing".

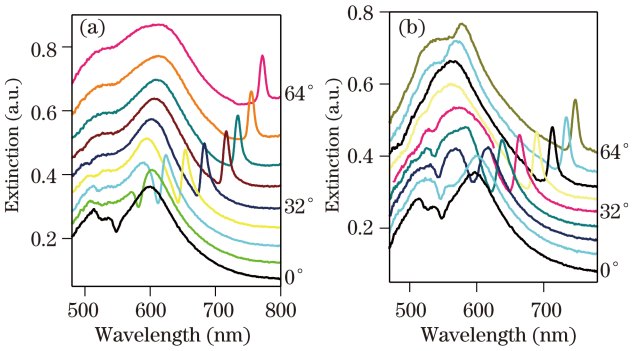

Fig. 2. Optical extinction spectra of the 2D gold MPC structures in Fig. 1(b) for (a) TM and (b) TE polarizations, respectively, with the incident angle varying from 0° to 64° in steps of 8°.

photoresist mask grating, which diffracts the incident light into the ITO layer to excite the waveguide mode. A 2D MPC fabricated by high temperature process is shown in Fig. 1(b). However, the periodicity of the 2D structures is a bit modified by the heating process and the 2D distribution becomes disordered to some extent. The nanocylinders have a period of about 330 nm and a mean diameter of about 130 nm.

The angle-resolved tuning properties of the waveguided 2D MPC structure are shown in Figs. 2(a) and (b) for the TM (in the incident plane) and TE (perpendicular to the incident plane) polarizations of the incident light, respectively. At normal incidence, coupling between the waveguide mode and the particle plasmon resonance of the gold nanocylinders can be observed at about 550 nm. With increasing the angle of incidence from 0° to 64°, the waveguide mode in the longer-wavelength branch is gradually tuned out of the spectral range of the particle plasmon resonance. The particle plasmon resonance is centered at about 600 nm for the TM polarization and about 570 nm for the TE polarization as estimated from Fig. 2. The enhanced transmission becomes extinction peaks in the optical extinction spectra when the angle of incidence is larger than 32° for the TM polarization and 40° for the TE polarization.

In the "pre-annealing lift-off" process, the sample that has been patterned with photoresist gratings and spin-coated with gold nanoparticle colloid is firstly heated by a hot plate at 150 °C for 5 min so as to decompose the ligands on the surface of the gold nanoparticles. After being cooled down to the room temperature, the sample is rinsed with acetone to remove the photoresist template. In the final stage, the sample is annealed at 250 °C on a hot plate for about 20 s to melt the gold nanoparticles and produce the 1D or 2D MPCs.

Figures 3(a) and (b) show the AFM images of the 1D and 2D MPCs fabricated by the "pre-annealing lift-off" process, where the positive photoresist S1805 is used to fabricate the template grating structures. The 1D MPC consists of periodically arranged nanowires with a period of 330 nm, as shown in Fig. 3(a). The nanowires are as high as 50 nm, which is controlled by the modulation depth of the photoresist gratings. The 2D MPC shown in Fig. 3(b) consists of square lattices of nanoholes and have a period of 330 nm. The nanoholes have a diameter of about 120 nm and a depth of about 60 nm. Further

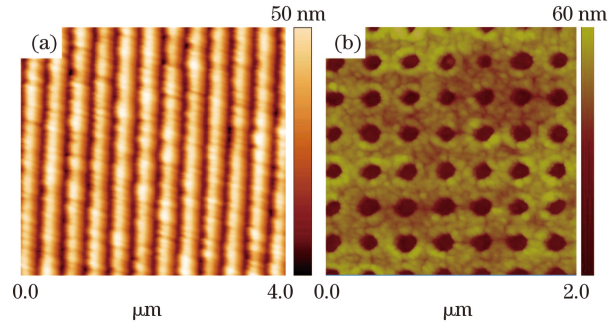

Fig. 3. AFM images of (a) 1D and (b) 2D gold photonic crystals with the photoresist mask grating removed through "pre-annealing lift-off".

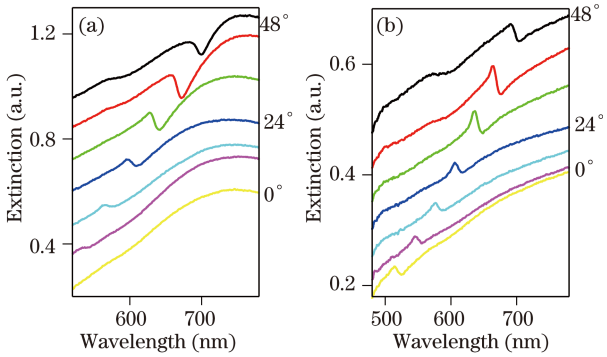

Fig. 4. Optical extinction spectra of the 1D gold photonic structures shown in Fig. 3(a) for (a) TM and (b) TE polarizations, respectively, with the incident angle increased from 0° to 48° in steps of 8°.

experimental work indicates convincingly that both the negative and the positive photoresists apply well to the "pre-annealing lift-off" method.

As an example, we show the angle resolved tuning properties of the optical extinction spectra of the 1D structure in Figs. 4(a) and (b) for TM and TE polarizations, respectively. Coupling between the waveguide mode and particle plasmon resonance of the nanowires can be observed for the TM polarization in the spectral range from 550 to about 700 nm when the incident angle is increased from 0° to 48°, which appears as a dip in the optical extinction spectra, as given in Fig. 4(a)[18,19]. Whereas only the resonance of the waveguide mode[20,21] can be observed in the range of 500–700 nm for the TE polarization when the incident angle is increased from 0° to 48°, which appears as the extinction peaks in Fig. 4(b).

In conclusion, we have demonstrated two modified solution-processsible methods for the fabrication of 1D and 2D MPCs, which involve the so-called "high-temperature annealing" and "pre-annealing lift-off" techniques. The photoresist mask grating has been removed successfully so that the photonic crystals consisting of pure gold nanostructures have been produced with excellent optical response. This improves the quality of the MPCs and enables potentially high signal-to-noise ratio in the applications including sensors.

This work was supported by the High-Tech Research and Development Program of China (No. 2007AA03Z306), the National Natural Science Foundation of China (No. 10774011), and the Beijing

Educational Commission (No. KZ200810005004).

References

1. X. P. Zhang, H. M. Liu, J. R. Tian, Y. R. Song, J. Y. Song, and L. Wang, Nano Lett. **8,** 2653 (2008).
2. X. P. Zhang, H. M. Liu, J. R. Tian, Y. R. Song, L. Wang, J. Y. Song, and G. Z. Zhang, Nanotechnol. **19,** 285202 (2008).
3. X. P. Zhang, B. Q. Sun, J. M. Hodgkiss, and R. H. Friend, Adv. Mater. **20,** 4455 (2008).
4. J. C. Yang, J. Ji, J. M. Hogle, and D. N. Larson, Nano Lett. **8,** 2718 (2008).
5. J. K. Prashant, W. Huang, and A. E. Mostafa, Nano Lett. **7,** 2080 (2007).
6. C. L. Haynes, A. D. McFarland, L. L. Zhao, R. P. Van Duyne, and G. C. Schatz, J. Phys. Chem. B **107,** 7337 (2003).
7. H. L. Chen, S. Y. Chuang, H. C. Cheng, C. H. Lin, and T. C. Chu, Microelectron. Eng. **83,** 893 (2006).
8. G. Zhang, J. Zhang, G. Xie, Z. Liu, and H. Shao, Small **2,** 1440 (2006).
9. B. D. Lucas, J. S. Kim, C. Chin, and L. J. Guo, Adv. Mater. **20,** 1129 (2008).
10. S. Cabrini, A. Carpentiero, R. Kumar, L. Businaro, P. Candeloro, M. Prasciolu, A. Gosparini, C. Andreani, M. DeVittorio, T. Stomeo, and E. DiFabrizio, Microelectron. Eng. **11,** 78 (2005).
11. J. Taniguchi, N. Ohno, S. Takeda, I. Miyamoto, and M. J. Komuro, J. Vac. Sci. Technol. B **16,** 2506 (1998).
12. S. Reyntjens and R. J. Puers, Micromech. Microeng. **10,** 181 (2000).
13. M. Ishida, J. Fujita, T. Ichihashi, Y. Ochiai, T. Kaito, and S. J. Matsui, J. Vac. Sci. Technol. B **21,** 2728 (2003).
14. X. P. Zhang, B. Q. Sun, R. H. Friend, H. C. Guo, D. Nau, and H. Giessen, Nano Lett. **6,** 651 (2006).
15. X. P. Zhang, B. Q. Sun, R. H. Friend, H. C. Guo, N. Tetreault, H. Giessen, and R. H. Friend, Appl. Phys. Lett. **90,** 133114 (2007).
16. H. C. Guo, D. Nau, A. Radke, X. P. Zhang, J. Stodolka, X. L. Yang, S. G. Tikhodeev, and N. A. Gippius, Appl. Phys. B **81,** 217 (2005).
17. M. J. Hostetler, J. E. Wingate, C. J. Zhong, J. E. Harris, R. W. Vachet, M. R. Clark, J. D. Londono, S. J. Green, J. J. Stokes, G. D. Wignall, G. L. Glish, M. D. Porter, N. D. Evans, and R. W. Murray, Langmuir **14,** 17 (1998).
18. A. Christ, S. G. Tikhodeev, N. A. Gippius, J. Kuhl, and H. Giessen, Phys. Rev. Lett. **91,** 183901 (2003).
19. S. Linden, A. Christ, J. Kuhl, and H. Giessen, Appl. Phys. B **73,** 311 (2001).
20. D. Rosenblatt, A. Sharon, and A. A. Friesem, IEEE J. Quantum Electron. **33,** 2038 (1997).
21. S. G. Tikhodeev, A. L. Yablonskii, E. A. Muljarov, N. A. Gippius, and T. Ishihara, Phys. Rev. B **66,** 045102 (2002).